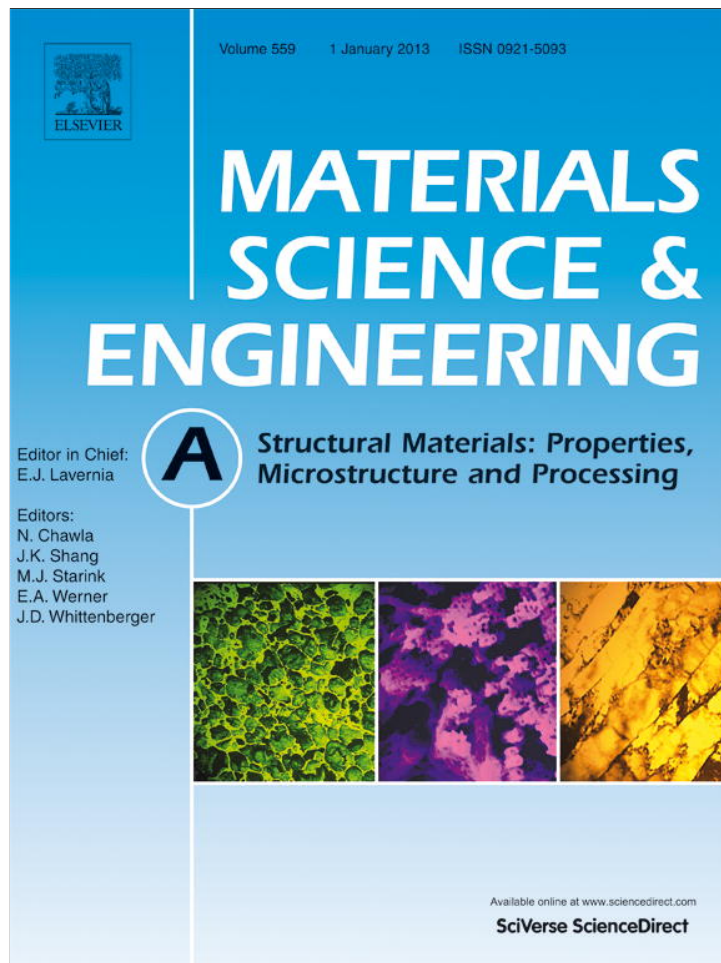


Provided for non-commercial research and education use.  
Not for reproduction, distribution or commercial use.



This article appeared in a journal published by Elsevier. The attached copy is furnished to the author for internal non-commercial research and education use, including for instruction at the authors institution and sharing with colleagues.

Other uses, including reproduction and distribution, or selling or licensing copies, or posting to personal, institutional or third party websites are prohibited.

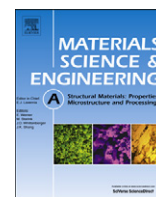
In most cases authors are permitted to post their version of the article (e.g. in Word or Tex form) to their personal website or institutional repository. Authors requiring further information regarding Elsevier's archiving and manuscript policies are encouraged to visit:

<http://www.elsevier.com/copyright>



Contents lists available at SciVerse ScienceDirect

## Materials Science &amp; Engineering A

journal homepage: [www.elsevier.com/locate/msea](http://www.elsevier.com/locate/msea)

## Microstructural, mechanical and fractographical study of titanium-CP and Ti-6Al-4V similar brazing with Ti-based filler

E. Ganjeh\*, H. Sarkhosh

Young Researchers Club, Tehran North Branch, Islamic Azad University, Tehran, Iran

## ARTICLE INFO

## Article history:

Received 19 July 2012

Accepted 11 August 2012

Available online 19 August 2012

## Keywords:

Mechanical characterization

Titanium alloys

Intermetallics

Brazing

Fracture

## ABSTRACT

Commercial pure titanium (Ti-CP) and Ti-6Al-4V alloy were brazed in a controlled atmosphere furnace, each of them to itself, using an amorphous STEMET 1228 (Ti-27Zr-14Cu-13Ni, wt%) brazing foil. Primarily, quality of the brazed joints was evaluated by an ultrasonic test and then effect of temperature and time were investigated on joint microstructure and mechanical properties. The former by metallography, scanning electron microscope (SEM) and X-ray diffraction (XRD) analyses and the latter by microhardness and shear test. Original microstructure of the Ti-CP and the Ti-6Al-4V base metals were not altered using this braze alloy. The joints mainly consist of  $\gamma$ -Cu/Ni [Ti(Zr)]<sub>2</sub> and  $\lambda$ -Lave (Cu/Ni)<sub>2</sub>[Ti,(Zr)] intermetallic compounds. Prolonging brazing time, results in replacement of these brittle phases with a fine acicular Widmanstätten structure dominating the entire joint due to redistribution of Cu and Ni from the braze alloy into the base metals. Optimum shear strength of the Ti-CP and the Ti-6Al-4V brazed joints were achieved 261.7 and 571 MPa, respectively. The best parameters for shear strength were obtained at 870 °C—30 min in case of the Ti-CP and 950 °C—30 min in case of the Ti-6Al-4V. Using Ti-26.8Zr-13.9Cu-13Ni amorphous filler alloy permits furnace brazing at a temperature lower than that of  $\alpha \Rightarrow \beta$  transformation. From practical point of view, it was found that controlled atmosphere brazing of compatible samples have located in a simple close chamber, maybe carried out as an effective and economic process.

© 2012 Elsevier B.V. All rights reserved.

### 1. Introduction

The light weight, high strength-to-weight ratio, and excellent corrosion resistance of titanium and its alloys such as Ti-6Al-4V have used in aerospace, chemical, marine industries and medical instruments [1,2]. Titanium and its alloys have used primarily in two areas of application where the unique characteristics of these metals justify their selection: corrosion-resistant service and strength-efficient structures [3,41]. Since titanium and its alloys do not react within the human body and are biocompatible, they have used to create artificial organs and other biological implants [4]. For the last half of the twentieth century, Ti-6Al-4V has been accounted for about 45% of the total weight of all titanium alloys shipped and its application in aerospace industries and biomaterial are approximately 33% because of good combinations of strength, toughness, corrosion and compatibility with polymer composite materials [3,5,6,41]. The major disadvantages of this metal and its alloys are its high cost and problems in joining. Similar joining titanium and its alloys is one of the main complications. All the

requirements for high quality joints and also reducing of needed materials will make economically attractive and viable if these joints successfully process [7]. Many titanium joining have employed processes such as welding, brazing and diffusion bonding [8,9]. Among those, titanium brazing technology extensively applies in aerospace industries and implantable biomedical manufacturing [10–12]. During the past decades, brazing of titanium and its alloys has become an important joining process to gain the increasingly demanding structural applications. Titanium brazing for elevated temperature services is frequently brazed with titanium and zirconium-based filler alloys which Cu and Ni are added as melting point depressants (MPDs) [13,14,41]. Erosion of the substrate and excessive growth of intermetallic compounds at interface will be significantly decreased or eliminated due to decline in brazing time or temperature. Recently, Ti-Zr base amorphous alloys are produced in ribbon shape in a wide variety of compositions using rapid solidification process (RSP). Serious efforts have been done to verify their characteristics as fillers for brazing of Ti and its alloys [14,15]. However, it is difficult to produce foils from fully alloyed Ti-Zr base filler alloys using plastic deformation technologies such as the rolling process, due to their main constituent phases are brittle [42]. Therefore, the Ti or Zr base filler alloys has used in the form of powders or

\* Corresponding author. Tel.: +98 2188674741.

E-mail address: [navidganjehie@sina.kntu.ac.ir](mailto:navidganjehie@sina.kntu.ac.ir) (E. Ganjeh).

amorphous foils produced by the RSP and have provided high joint strength and good corrosion resistance in comparison with other type of brazing fillers such as Ag or Al base filler alloys. The Ti–Zr base filler alloys are produced by the RSP, can have homogeneous microstructure [13,14,16,17]. Brazing technique used in joining titanium and its alloys is a significant factor [9]. For titanium brazing, furnace brazing is an ideal industry process in an inert atmosphere or vacuum. Many investigations have been done [8,14,18–20] on brazing the Ti–CP and the Ti–6Al–4V with Ti-based filler alloys.

Botstein et al. [21] reported a good strength of Ti–6Al–4V joints brazed by 25Ti–25Zr–50Cu amorphous filler alloy using vacuum furnace brazing. It was concluded that a fine lamellar eutectic structure was formed after 950 °C–10 min, which was a mixture of  $\gamma$ -Cu[Ti(Zr)]<sub>2</sub> tetragonal and  $\alpha$ -Ti phases. Also, a coarse dendritic structure was crystallized at the center of the joint which its main constituent was hexagonal  $\lambda$  (Laves phase) Cu<sub>2</sub>TiZr and  $\gamma$  phases. When the formation of the brittle  $\lambda$  Laves phase was suppressed by a fast heating and cooling regime of brazing operation, high joint mechanical properties were obtained.

At the other study was conducted by Iijima and colleagues [22], infrared brazing of beta-titanium wire (Ti–11Mo–6Zr–4Sn) by Ti–30Ni–20Cu braze alloy had investigated. They found that titanium in diffusion layer has an irregular concentration gradient in which the braze alloy side has a higher concentration. Distribution of Sn atoms was very similar to that of Cu or Ti in the diffusion layer, which was corresponding to formation of Cu–Ti and Cu–Sn intermetallic compounds.

The goals of this study are divided into three sections. First, appropriate brazing conditions for optimal mechanical properties of the joints were determined. Then, phase analyses of the joint microstructure to establish a relation between microstructure and mechanical properties were investigated. Finally, a comprehensive study was done to describe the fracture modes ascribe to fractography results.

## 2. Experimental procedures

Sheets of Ti–CP (ASTM Grade 2) with 1.5 mm and Ti–6Al–4V (ASTM Grade 5) with 3 mm in thickness were used as base metals in this study. The mechanical properties of base metals are mentioned in Table 1. Single lap shear specimens of both base metal sheets were prepared using a wire-cutting machine followed by brazing with an overlapping of 3T according to JIS Z 3192 [23] standard. Then, these specimens were polished with wet SiC papers up to 600 grit and subsequently were cleaned by an ultrasonic bath with acetone as the fluid before brazing. Also, the plates were cut into 10 × 15 mm chips for microstructure analysis. A near eutectic Ti–27Zr–14Cu–13Ni (wt%) brazing foil (STEMET 1228) with 50  $\mu$ m thickness was used as the brazing filler alloy. This brazing foil has solidus and liquidus temperature of 664 and 825 °C, respectively. The brazing foil was cleaned by acetone before brazing and then sandwiched between the overlapped areas of the parent metals and carefully was placed into a controlled atmosphere furnace.

Furnace brazing was conducted in an argon atmosphere. The heating and cooling rates during the brazing cycles were adjusted

**Table 1**  
Mechanical properties for the Ti–CP and the Ti–6Al–4V base metals.

Base metal	Yield strength (Mpa)	Tensile strength (Mpa)	Elongation (%)
Ti–CP $\alpha \rightarrow \beta$ Temp=890 °C	345	433	22
Ti–6Al–4V $\alpha \rightarrow \beta$ Temp=1015 °C	950	1010	14

at 65 °C/min. The setting up and procedure of the brazing process has described in details in our previous publications [24,41].

The ultrasonic test was carried out by using a probe of focusing type generating a longitudinal wave of 22 MHz. Measurements were performed on thickness measurement “Krautkramer Branson” according to AWS C3.8 [25] developed at Iran Air Organization with a standard CL3 DL (Transducer: Alpha, Aerotech) which was attached to the surface of the brazed joint.

Standard grinding and polishing sample preparation procedure was applied [26] and Kroll's reagent was used to evaluate the microstructures by light optical microscope (LOM). The cross-sections of the brazed specimens were investigated with a VEGA/TESCAN scanning electron microscope (SEM). The quantitative chemical composition analysis of the brazed joints was conducted using an energy dispersive spectrometer (EDS). The shear test was performed to evaluate the bonding strength of the brazed joints using a Zwick/Reoll Hct 400/25 dynamic testing machine with a constant crosshead speed of 0.5 mm/min [15,24]. At least two shear test specimens were performed for each brazing condition. Vickers microhardness indentation measurement (7 points) was performed to evaluate the different phases formed in the joints which were measured by a 100-g load and a duration time of 35 s and repeated for three times in each point. Therefore, the mean values were taken in order to assure validity of the results. First, fractured surfaces were examined by an SEM followed by a structural analysis. The structure analysis was performed using a Philips PW 1800 X-ray diffractometer (XRD). Cu K<sub>α1</sub> was selected as the X-ray source. The X-ray scan rate was set at 0.02°/s and its range was between 20° and 110°.

## 3. Results and discussion

### 3.1. Ultrasonic test

According to ultrasonic test, sound joints were obtained without any voids or cracks along joints which brazed at temperatures of 870 °C (Ti–CP samples) and 950 °C (Ti–6Al–4V samples) as have demonstrated in Table 2. According to Table 2, samples which brazed at temperature of 850 °C for Ti–CP and 900 °C for Ti–6Al–4V have rejected. Hence, our studies have focused for accepted samples.

### 3.2. Microstructural evolution of Ti–CP brazed joints

Fig. 1 shows SEM backscattered electron images (BEIs) and EDS chemical analysis (Table 3) results in atomic percent of furnace brazed Ti–CP samples in the different regions with Ti–27Zr–14Cu–13Ni foil at temperature of 870 °C. Two distinctive regions were observed in brazing experiments: appearance of a phase along the central line of the joint (Zr–Cu–Ni segregated region) and an

**Table 2**  
Results of the ultrasonic test for furnace brazed joints.

Base metal	Temp. (°C)	Time (min)	Layer thickness (mm)	Joint thickness (mm)	Results
Ti–CP	850	10	1.49	1.49	Rej.
	850	30	1.51	1.51	Rej.
	870	10	1.52	3.03	Acc.
	870	20	1.52	3.03	Acc.
Ti–6Al–4V	870	30	1.5	3.04	Acc.
	900	10	3.00	3.00	Rej.
	900	30	3.01	3.01	Rej.
	950	10	3	5.68	Acc.
	950	20	2.9	5.9	Acc.
	950	30	3.1	6	Acc.

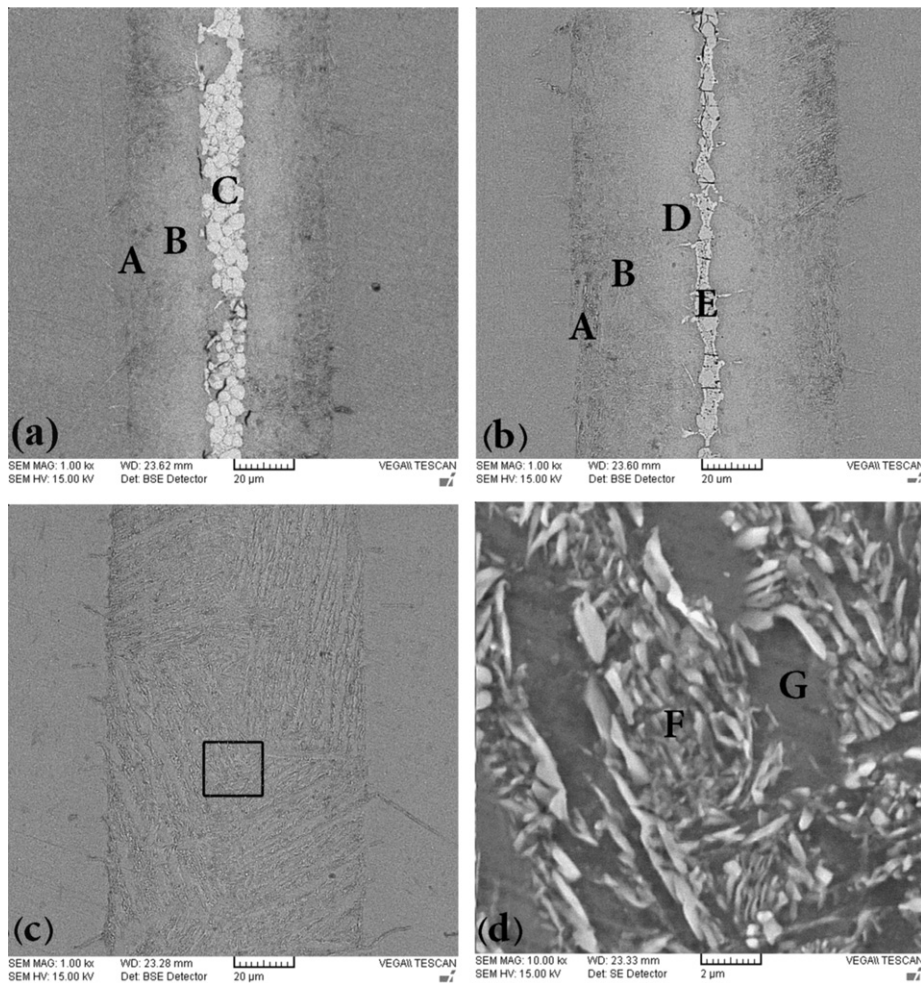


**Fig. 1.** SEM-BEIs microstructure features of the Ti-CP samples brazed at temperature of 870 °C for (a) 10 min, (b) 20 min and (c) 30 min; (d) closer view of the rectangular area in (c).

**Table 3**  
Chemical analyses at regions shown in Fig. 1.

Symbol	Chemical analyses (at%)				Potential phase(s)
	Ti	Zr	Ni	Cu	
A	93.4	1.4	2.4	2.8	$\alpha$ -Ti
B	87.3	4	3.4	5.3	$(\alpha\text{-Ti}) + (\text{Ti,Zr})_2\text{Ni} + (\text{Ti,Zr})_2\text{Cu}$
C	51.9	12.4	19.2	16.5	$(\text{Ti,Zr})\text{Cu}_2, (\text{Ti,Zr})_2\text{Ni}, (\text{Ti,Zr})_2\text{Cu}$
D	80.8	7.9	7.6	3.7	$(\alpha\text{-Ti}) + (\text{Ti,Zr})_2\text{Ni} + (\text{Ti,Zr})_2\text{Cu}$
E	60.5	10.8	10.7	18	$(\text{Ti,Zr})\text{Cu}_2, (\text{Ti,Zr})_2\text{Ni}, (\text{Ti,Zr})_2\text{Cu}$
F	86.4	3.8	3.1	6.7	$\beta$ -Ti
G	95.2	3	0.8	1	$\alpha$ -Ti

acicular region close to the base metal as shown in Fig. 1(a) to (c). The last one was received when the brazing time reached to 30 min. Fig. 1(c) and (d) denotes the microstructure has been uniform in element distribution when brazing time has increased up to 30 min. This characteristic is related to atomic diffusion phenomena such as isothermal solidification and solid-state diffusion during brazing [22,27].

As a result of Fig. 1(a) and (b), region A is a Ti-rich phase which alloyed with some alloying elements in filler metal like Cu, Ni and Zr. The interfacial zones have relatively high (> 80 at%) titanium content and low Ni, Cu and Zr concentrations (regions B and D). The high contain of Ti and small amounts of Ni, Cu and Zr are responsible for developing the  $(\alpha\text{-Ti}) + (\text{Ti,Zr})_2\text{Ni} + (\text{Ti,Zr})_2\text{Cu}$  fine

eutectoid microstructure. These phases should be the results of reaction dissolving elements of base metal with alloying components in liquid filler alloy. The central regions which are marked by C and E have more than 50 at% Ti and high nickel, copper and zirconium contents. Relevant to Fig. 1(c) and (d), as the brazing time increased to 30 min, the central regions were disappeared and only a primary crystal with aciculate microstructure were observed at the interface. This microstructure was formed by isothermal solidification with diffusion of the lower melting point (Cu and Ni) elements into the base metal [15]. Similar microstructure was observed on the brazed joint with Zr–13.8Ti–10Ni–12.5Cu–22.5Be filler alloy at 800 °C–10 min [27] and also on the brazed joint by Ti–24Zr–16Cu–16Ni powder blend 900 °C–15 min [28]. Consequently, brazing at 870 °C–30 min would promote the formation of an acicular Widmanstätten structure. This microstructure is similar to  $\alpha + \beta$  phase titanium [3].

### 3.3. Microstructural evolution of Ti–6Al–4V brazed joints

Fig. 2 shows SEM-BEIs and EDS chemical analysis results (Table 4) in atomic percent of the furnace brazed Ti–6Al–4V using the Ti–27Zr–14Cu–13Ni foil at temperature of 950 °C for 10, 20 and 30 min. The interface between Ti–6Al–4V and the braze alloy is free of a continuous reaction layer. The characteristic regions are formed by interdiffusion and solubility limits, including isothermal solidification and solid-state diffusion during brazing [22]. Based on the microstructural morphology and the chemical composition, four

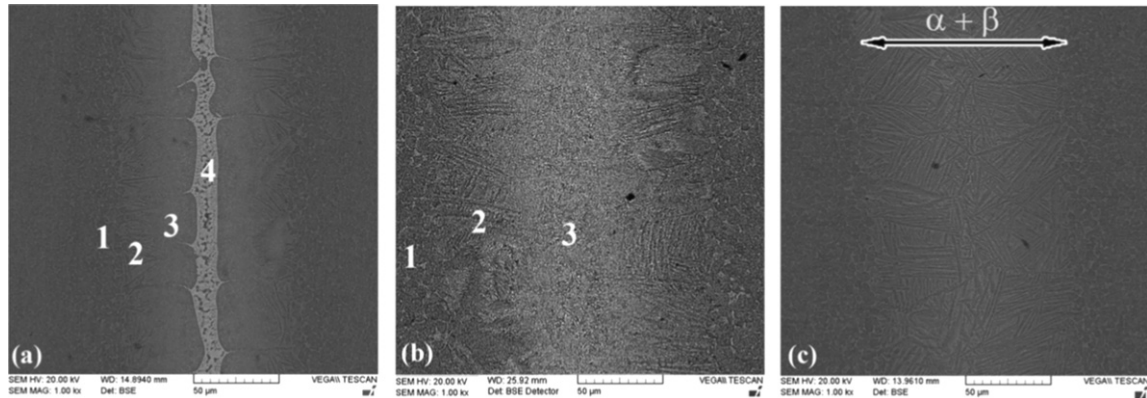


Fig. 2. SEM BEI microstructure features of the furnace brazed Ti-6Al-4V using Ti-27Zr-14Cu-13Ni braze alloy at 950 °C for: (a) 10 min; (b) 20 min and (c) 30 min.

Table 4  
Chemical analyses at regions shown in Fig. 2.

Symbol	Chemical analyses (at%)						Potential phase(s)
	Ti	Al	V	Zr	Ni	Cu	
1	85	6.2	3.7	1	2	2.1	Equiaxed $\alpha + \beta$ phase (Ti-6Al-4V)
2	78.6	9.7	2.3	2.1	4.9	2.4	Acicular $\alpha + \beta$ Ti
3	76.8	6.2	0.3	3.7	6	7	( $\alpha$ -Ti)+Cu-Ni in Ti-rich
4	54.5	2.9	1	12.4	14	15.2	(Ti,Zr)Cu <sub>2</sub> , (Ti,Zr) <sub>2</sub> Ni, (Ti,Zr) <sub>2</sub> Cu

different types of the joint microstructures were observed. The formation of these regions indicates that a strong reaction of the molten filler alloy with the Ti-6Al-4V base metal have carried out during brazing. Similar to cross-section images of the brazed joint in the Ti-CP (Fig. 1(a) and (b)), brazed samples at temperature of 950 °C—10 and 20 min are primarily composed of Ti-rich phase alloyed with Ni, Cu and Al as labeled by 1–3 in the Fig. 2(a) and (b). During brazing, in the region 2, diffusion of Cu and Ni atoms from the liquid filler alloy into the original equiaxed  $\alpha$  plus intergranular  $\beta$  base metal, transformed the structure into the  $\beta$  phase because of the Cu and Ni elements are the  $\beta$ -Ti stabilizers in the Ti-6Al-4V alloy. Region 3 has a eutectoid microstructure containing Ti and a small amount of Ni, Cu and Zr at the base metal side and is comprised of (Ti,Zr)<sub>2</sub>Ni and (Ti,Zr)<sub>2</sub>Cu phases. As the brazing time increases to 20 min at temperature of 950 °C, the central brazed layer disappears and only the eutectoid regions could be observed in the solid solution matrix of Ti. The composition of region 4 is almost identical to the original filler alloy. According to EDS analysis results, region 4 consists of a large amount of Ti-Ni-Cu and Zr intermetallic compounds, which these phases should be (Ti,Zr)<sub>2</sub>Ni, (Ti,Zr)<sub>2</sub>Cu as  $\gamma$  and (Ti,Zr)Cu<sub>2</sub> as  $\lambda$  Lave phases. As illustrated in Fig. 2(c), cooling from  $\beta$  phase at high temperature is responsible for nucleation of acicular  $\alpha$  phase which leaved untransformed  $\beta$  phase on its grain boundaries [29].

At the early stage of brazing, the Ti-6Al-4V base metal dissolves considerably into the molten filler alloy. As a result, the molten filler in the vicinity of the Ti-6Al-4V base metal has become richer in Ti. The primary isothermally solidified phase is the  $\alpha$ -Ti rather than the  $\beta$ -Ti, (Fig. 3(a)) as the brazing temperature is lower than the  $\alpha$ - $\beta$  transformation temperature. When the  $\alpha$ -Ti phase nucleates and grows into the joint as illustrated in Fig. 3(b), excessive Ni and Cu atoms are expelled from the growing  $\alpha$ -Ti phase and segregate at the central region. The solubility of Cu and Ni in  $\alpha$ -Ti is much lower than that in  $\beta$ -Ti [30]. So, transformed  $\beta$ -Ti phase is formed at segregated region, as the Cu and Ni elements are  $\beta$ -Ti stabilizers. Finally, the absence of  $\beta$ -Ti phase in the brazed joint is rationalized by the eutectoid decomposition of this phase to fine lamellar  $\alpha$ -Ti and  $\gamma$

phases ( $\beta$ -Ti  $\rightarrow$   $\alpha$ -Ti + (Ti,Zr)<sub>2</sub>Ni + (Ti,Zr)<sub>2</sub>Cu) at the subsequent cooling stages.

This selective nucleation and growth mechanism leads to formation a characteristic microstructure that is called “Widmanstätten or acicular” structure [29]. The needle like feature is caused by rapid cooling with a rate of 65 °C/min from brazing temperature to medium (Fig. 3c). The formation of the acicular structure in both joints can be explained by the isothermal solidification that occurred during brazing. This microstructure was the same, when the Ti-6Al-4V furnace brazed with STEMET 1406 (Zr-9.7Ti-12.4Ni-11.2Cu, wt.%) amorphous filler alloys at 990 °C – 30 min [41].

It is worth to note that the same Widmanstätten structure in both joints are established during 30 min brazing cycle but at temperature of 870 °C for the Ti-CP and 950 °C for the Ti-6Al-4V base metals. The relation between two different temperature brazing can be discussed using the concept of surface energy (or bonding strength between atoms in a crystal structure). The brazing process depends on liquid metal flowing over a surface to forms reactionary layers into the gap between the components to generate a permanent bond. Brazing is a diffusion base process which the melting temperature of alloying elements in filler alloys, activates this phenomenon. After the melting of filler alloy, many parameters are influenced in diffusion among grain boundaries. Clearness and surface preparation conditions (mechanical or chemical) are the main factors to control the wetting occurrence. Wettability is only a function of the free energy change of the surface. The roughness of solid surfaces affects the wetting owing to two different reasons: the first is the fact that the actual surface area is increased and the second is pinning of the triple line by sharp edges [31]. There is an optimum surface roughness which could be achieved by mechanical polishing (SiC abrasive paper from 100 to 600) according to Hong and Koo [32] results. A rough surface can change the flow mode of the liquid filler alloy from laminar to turbulent, improving the interaction between the filler alloy and the substrate [31,32]. A general equation for modeling the wetting of filler alloy on a substrate is proposed by Young [31,33] as shown in Fig. 4 and Eq. (1):

$$\cos \theta = \frac{\gamma_{SV} - \gamma_{LS}}{\gamma_{LV}} \quad (1)$$

where  $\theta$  is the contact angle,  $\gamma_{LV}$  is the liquid/vapor interfacial energy,  $\gamma_{SV}$  is the solid/vapor interfacial energy, and  $\gamma_{LS}$  is the liquid/solid interfacial energy. In both brazing systems, the chemical composition of filler alloy is the same so, the  $(\gamma_{LV})_{Ti-CP} - (\gamma_{LV})_{Ti-6Al-4V}$ . Consequently, the Eq. (1) summarized to:

$$\frac{(\cos \theta)_{Ti-CP}}{(\cos \theta)_{Ti-6Al-4V}} = \frac{(\gamma_{SV} - \gamma_{LS})_{Ti-CP}}{(\gamma_{SV} - \gamma_{LS})_{Ti-6Al-4V}} \quad (2)$$

Liquid alloys wet well solid substrates ( $\theta \ll 90$ ), unless the solid surfaces subjected to oxidization. Adsorption of oxygen on

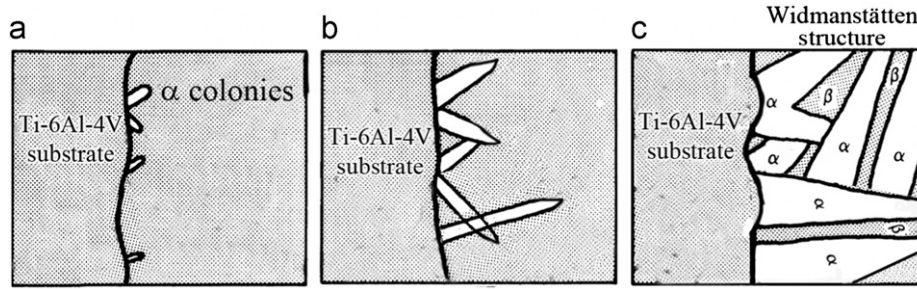


Fig. 3. Different steps of diffusion of  $\alpha$  colonies at interface during brazing; (a) nucleation of  $\alpha$ -Ti at interface, (b) growth of  $\alpha$  phases into braze joint and (c) final microstructure which contained plates of  $\alpha$  separated by the  $\beta$  phase.

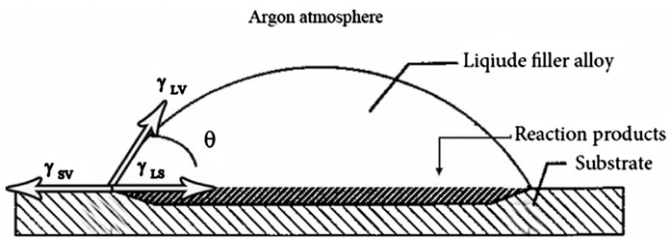


Fig. 4. Schematic illustration for wetting [31].

solid substrates could increase contact angles. Intrinsic wetting seems to be slightly improved in systems with some solubility or form intermetallics. Furnace brazing using controlled atmosphere in inert gases (generally Ar or He) or vacuum, can be used to achieve environments in which flow is unrestrained by oxide skins and component surfaces are clean metals. It should be stated that abrasion paper changes the topography of surfaces as well as the chemistry by removing oxide films. Liquid will flow into the joint, if the braze wets the component materials. Afterward, the good diffusion achievement is function of configuration of braze jigs and the joint design. The principle factor for advancing molten filler alloy on substrate is ascribed to  $\gamma_{SV}$  until it wets entire braze surface [34]. Finally, the Eq. (2) has changed to below:

$$\frac{(\cos \theta)_{Ti-CP}}{(\cos \theta)_{Ti-6Al-4V}} = \frac{(\gamma_{SV})_{Ti-CP}}{(\gamma_{SV})_{Ti-6Al-4V}} \quad (3)$$

The  $\gamma_{SV}$  (known as surface energy) has opposite relation with contact angle ( $\theta$ ). The surface energy is the work required to form a unit area of surface. In addition, it is the energy required to transform a bulk atom into a surface atom with a corresponding increase in the surface area. Surface energy is one of the most fundamental parameters of solids, since it depends directly on the bonding forces of the material atoms [35]. Experimental measurement of solid surface energy is out of the paper scope, duo to difficulties of measurement and interpretation. In a research work that was done by Roth and Suppayar [36], the surface energy of both the Ti-CP and the Ti-6Al-4V were measured at temperature of 1138–1315 °C. The results indicated that the  $(\gamma_{SV})_{Ti-CP}$  is less than the  $(\gamma_{SV})_{Ti-6Al-4V}$  with a difference of approximately 100 erg/cm<sup>2</sup> (mJ/m<sup>2</sup>). Accordingly, the more surface energy means more energy needs (heat) for cutting the atom bonds in a crystal structure for activating them to do reaction. In a point of view to bonding energy of compounds [37], Ti-V bonding energy in the Ti-6Al-4V substrate is the strongest bond between Ti-Al and the Ti-CP base metal owing to the high melting temperature of vanadium. On the other hand, at a same temperature, the greater surface energy means (Eq. (3)) the greater wettability angle for the Ti-6Al-4V in comparison to the Ti-CP. Therefore, increasing the 80 °C in brazing temperature for the Ti-6Al-4V

substrate for generating the same microstructure is associated to these metallurgical and chemical matters.

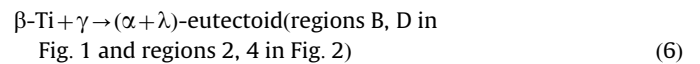
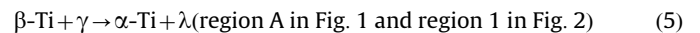
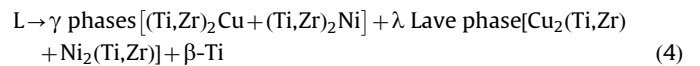
### 3.4. Evolution of reaction mechanism

To understand the genesis of different brazed microstructures during the brazing, some logical assumes should be attributed as below:

- 1- The Cu atoms act as Ni ones in the joint, as they are both  $\beta$ -Ti stabilizers with similar atomic size and structure and form isomorphous solutions in both solid and liquid phases [15]. Therefore, Ti-Zr-Cu ternary alloy phase diagram (Fig. 5(a)–(d)) at isothermal sections of 925, 875 and 827 °C is cited here in order to unveil microstructural evolution of the furnace brazed joints.
- 2- The Al and V are soluble in the titanium substrate and do not form any intermetallic compound.

The transformation of the  $\beta$ -Ti phase upon cooling cycle of brazing significantly has complicated microstructure in the brazed joint, using Ti-based brazing alloy. As noted from the Ti-Zr-Cu ternary alloy phase diagram (Fig. 5), the Ti<sub>2</sub>Cu or Ti<sub>2</sub>Ni phases have some solubility of Zr. Therefore, the brazed joint consists of (Ti,Zr)<sub>2</sub>Cu, (Ti,Zr)<sub>2</sub>Ni and  $\beta$ -Ti phases upon further cooling from 925 to 827 °C.

Subsequently, the joint microstructures may be formed as a result of both crystallization into  $\beta + \gamma$ -(Ti,Zr)<sub>2</sub>Cu/Ni peritectic or into  $\gamma + (\lambda$ -Laves [Cu/Ni]<sub>2</sub>(Ti,Zr) phase) eutectic [20]. Cooling from low brazing time leaves  $\gamma + \lambda$  eutectic untransformed. On the other hand, solidification of the molten braze experiences various mixtures of phases containing  $\alpha$ -Ti,  $\gamma$  and  $\lambda$  phases upon cooling cycle of brazing. These stages (reactions) can be presented as Eqs. ((4)–(7)):



Based on Eqs. (4)–(7), the consumption of (Ti,Zr)<sub>2</sub>Cu, (Ti,Zr)<sub>2</sub>Ni, (Ti,Zr)Cu<sub>2</sub> and  $\beta$ -Ti phases yield Widmanstätten structure. The presence of the equilibrium phases can be predicted from these phase diagrams. However, the morphology of various phases in the joint cannot be determined from the phase diagram, individually. The transformation kinetic always plays an essential role in determining final microstructure in the Ti brazed joint. For instance, the redistribution of Cu, Ni, Zr (from the braze alloy) and Al, V (from the Ti-6Al-4V substrate) in the furnace brazed joint

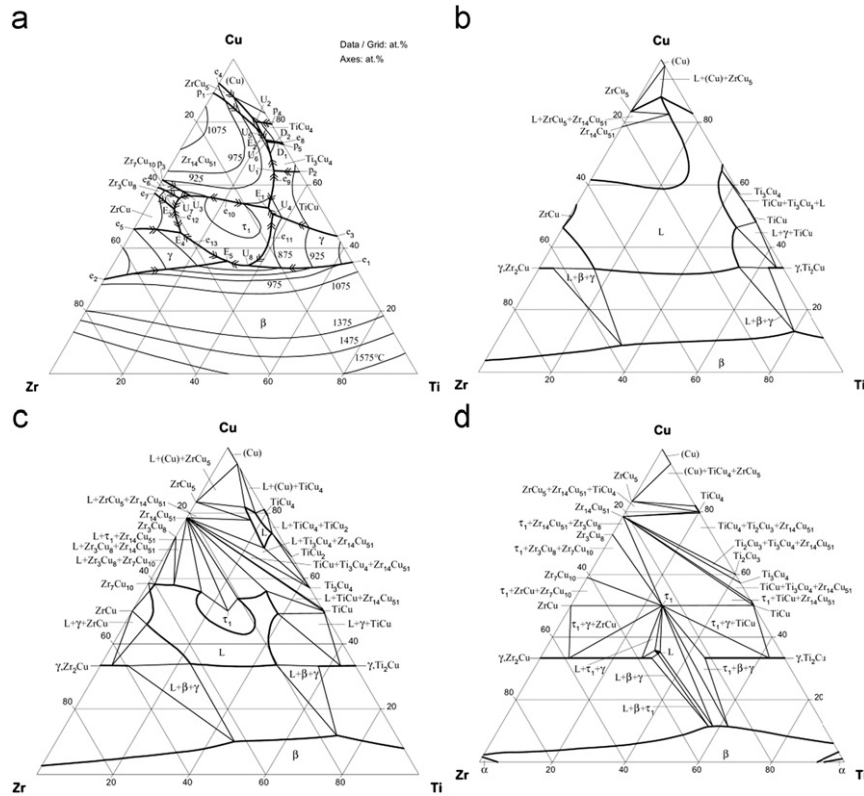


**Fig. 5.** Ti–Zr–Cu ternary alloy phase diagram; (a) liquidus projection with liquidus isotherms, surface of primary solidification in isothermal section at (b) 925 °C, (c) 875 °C and (d) 827 °C [19].

greatly change the transformation of the  $\beta$ -Ti phase upon cooling cycle of the brazing. Al element is the only  $\alpha$  stabilizer for the Ti alloy. All other elements such as Cu, Ni and V are the  $\beta$  stabilizers [38]. Cu–Ti and Ni–Ti are categorized as the  $\beta$  eutectoid systems. In contrast, V in Ti belongs to the  $\beta$  isomorphous system. Accordingly, it is possible that the  $\alpha + \beta$  Ti be stabilized at room temperature by these alloying elements. At the onset of the isothermal solidification, the solid/liquid (S/L) interface is unstable due to the dissolution effect of the base metal, so the Ti solid solution layer has an irregular interface with the base metal. As more Cu atoms diffuse into the primary layer, a new Ti solid solution layer with a fine lamellar structure started to grow into the joint. Subsequently, these dendritic phases directionally grow into the joint according to the diffusion path of the alloying elements. These two regions continued to grow into the joint and finally encounter with each other's. At this moment, the molten liquid has completely consumed, and the eutectic regions are hardly observed.

### 3.5. Mechanical properties of the joints

#### 3.5.1. Shear strength

Fig. 6 shows the mechanical properties of the Ti-CP brazed specimens with various brazing times. The test results revealed that the shear strength of the Ti-CP specimens which are brazed with STEMET 1228 at 870 °C enhances with increasing the brazing time, except at 20 min. The lowered strength is related to microstructure feature as shown in Fig. 7. From a microstructural point of view, variations in joint strength with the brazing parameters depend noticeably on the joint microstructure. As the brazing time becomes lower the central brazed layer would remain in the brazed joint and the shear strength dwindled significantly (112.8 MPa) until fracture occurs in the central brazed layer which is contained of  $\lambda$  and  $\gamma$  brittle intermetallic compounds. Botstein et al. [20] demonstrated that the  $\lambda$ -Lave phase are more detrimental for shear strength at

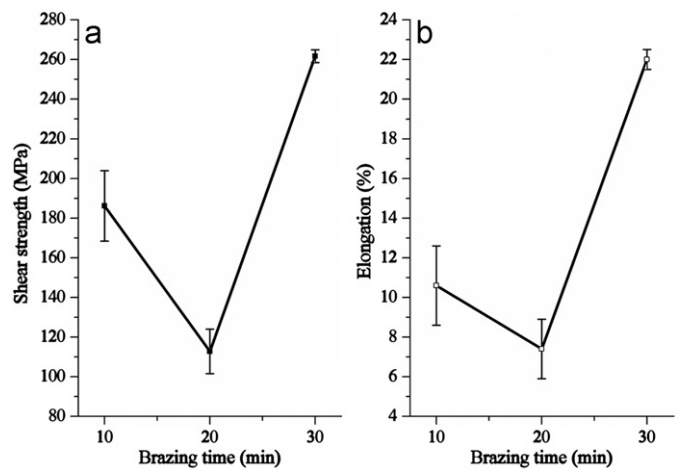


**Fig. 6.** Data obtained from stress-strain curves for shear strength (a) and elongation (b) for the Ti-CP brazed joint at different brazing time for temperature of 870 °C.

brazed joint. Summarizing, brazing conditions should be designed to avoid formation of  $\lambda$ -Lave brittle phase. This would be achieved if copper concentration in the center of the joint after completion of the brazing operation is within the  $7 < Cu < 14$  wt% range.

Prolonging the brazing time to 30 min causes the joints fracture in the base metal. However, increasing the brazing time or temperature led to more wetting, interaction or mutual diffusion at the interface which reflects high strength of the joint. Therefore, it has concluded that the brazed joint in this brazing condition has equal strength with the base metal. It is well known that the shear strength is  $\sim 0.6$  of maximum tensile strength [39]. However, these results have good agreement with furnace brazing of the Ti-CP with Ti–37.5Zr–15Cu–10Ni as a filler alloy at

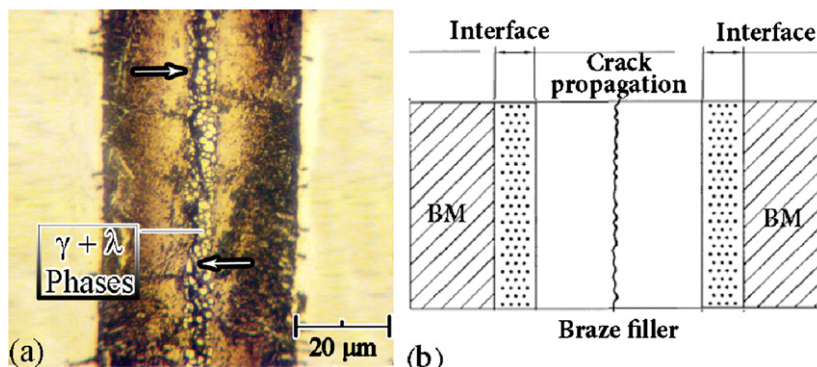


Fig. 7. (a) The LOM microstructure of the Ti-CP substrate which brazed at temperature of 870 °C for 20 min with STEMET 1228 filler alloy and (b) a model for describing the crack route.

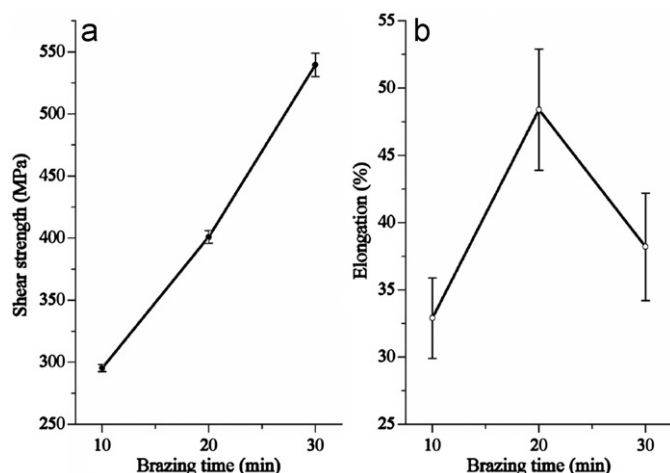


Fig. 8. Data obtained from stress–strain curves for shear strength (a) and elongation (b) for the Ti–6Al–4V brazed joint at different brazing time for temperature of 950 °C.

880 °C—30 min [18]. Therefore, to obtain the sufficient shear strength for brazing the Ti-CP with STEMET 1228, eliminating of the central brazed layer consisting of brittle intermetallic compounds is necessary. Finally, mechanical properties which are achieved from the shear test revealed that the brazing of the Ti-CP by STEMET 1228 has more strength in compare with brazing of the Ti-CP by Ag-based filler alloy which was conducted in our previous paper [24].

Same results have gained from stress–strain curves of the Ti–6Al–4V braze joints as denoted in Fig. 8. It is worth to note that brazing for 20 min generates a higher elongation in comparison to the others times. Developing a eutectoidal structure (Fig. 2(b)) creates high strength and higher elongation. Samples which consist only fine eutectoidal and Widmanstätten + eutectoidal microstructures have high elongation and exhibit ductile behavior [20]. The specimens brazed at temperature of 950 °C for 10 min have the lowest shear strength of 292 MPa with an elongation of 33%. When the brazing time is increased to 20 min the strength increases almost 1.5 times (403 MPa) and 48% for elongation. Increasing time to 30 min caused to achieve highest shear strength of 540 MPa but elongation decreased to lowest value namely 30% and the fracture has propagated in the base metal instead of through the brazed joint. Therefore, the shear strength of the specimens brazed at temperature of 950 °C increases with increasing the brazing time and the joints are fractured in the base metal for the brazing time of 30 min. The elongation of these samples is even better than that

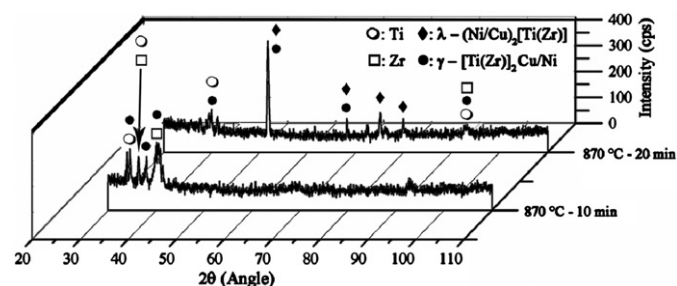


Fig. 9. XRD patterns from the Ti-CP fractured surface at brazing temperatures of 870 °C for 10 and 20 min.

elongation of the original base metal, probably due to their partial stress relaxation during brazing cycle.

The most important feature of samples microstructure after brazing under mentioned conditions is the absence of any changes in the base metals microstructure. This reality indicates that the changes in the alloy concentration during brazing cycles are not sufficient to induce changes into the base metals phase structure or to promote the grain growth. The absence of any changes in the surface area of the samples indicates that no overheating has occurred.

To verify phases developed in the Ti-CP brazed joints, X-ray diffraction analysis was done on the fractured surfaces after the shear test. The XRD analyses from fractured surfaces which brazed by STEMET 1228 at 870 °C—10 min and 870 °C—20 min are shown in Fig. 9. Several intermetallic compounds such as  $\gamma$ -[(Ti,Zr)<sub>2</sub>Cu/Ni] and  $\lambda$ -(Ni,Cu)<sub>2</sub>[Ti,(Zr)] were detected and confirmed by XRD analysis. According to Fig. 9, peak intensity of the intermetallic phases (such as  $\lambda$  and  $\gamma$ ) in specimen brazed at 870 °C—10 min were lower than the specimen brazed at 870 °C—20 min, which represents decline in volume percent of this phases and homogenized distribution. Therefore, lowering brittle intermetallic compounds especially the Laves phases are the main reason for increasing the joint strength. Hence, inordinate formation of brittle intermetallic phases (copper-based) is the mainspring of fracture.

It was reported that the amount of Cu–Ni rich Ti phase strongly related to the strength of brazed joint [17]. The effect of Cu–Ni–Zr rich Ti phases on braze joint strength using Ti–Zr–Cu–Ni filler alloy will be evaluated in this experiment to identify.

Fig. 10 displays the XRD results of fractured surfaces for the Ti–6Al–4V samples which were brazed by STEMET 1228 in temperature of 950 °C for 10 and 20 min. Several intermetallic compounds detected same as guesstimated in the microstructural analyses. Accordingly, when brazing time increases to 20 min at temperature of 950 °C, the peak intensity of intermetallic compounds such as Cu–Ni–Zr rich Ti phases decreases rather than 10 min.

At low brazing time, the intermetallic phases such as  $\gamma$  and  $\lambda$  Lave phases have been dominated. Moreover, the  $\lambda$ -Lave phase was detected in the microstructure analysis. It is found that TiCu intermetallic phase is clearly detected from fracture surfaces but with lower peaks, which could be owing to their low volume fraction. Based on the X-ray analysis, when the brazing time prolonged to 20 min, these phases dissolved among the brazed joint in so far as that the peak's intensity lowered and the titanium solid solution was contained some of these intermetallics compounds on the fracture surface. It means that fracture has occurred from braze interface, not at center area. It indicates that the interfacial layer between the Ti-6Al-4V and the braze alloy has played a crucial role in bonding strength of the joint. Formation of brittle  $\lambda$ -Lave phase has caused a drastic downfall in the strength of the brazed samples. Indeed, the samples which have exhibited a coarse, two phased  $\alpha$ -Ti+ $\lambda$ -Lave dendritic microstructure causing formation of multiple cracks within the joints upon shear test [20].

3.5.2. Microhardness measurement

The Vickers microhardness of different zones for both substrates brazed joints with STEMET 1228 are collected in Table 5. Microhardness indentation measurements are performed to evaluate the different phases formed in the joints. The Ti-CP brazing at temperature of 870 °C for 10 and 20 min, has shown the highest microhardness value (720–730 HV) which ascribe to brittle intermetallic compounds remained at the center of brazed joints with same chemical composition to original STEMET 1228 filler alloy. Appearance of Ti-rich phase developed average hardness of 380–480 HV attributed to eutectoid microstructure containing amount of Ni, Cu and Zr. Brazing at temperature of 870 °C for 30 min established an acicular Widmanstätten structure with uniform hardness distribution of 460–500 HV which was higher than the Ti-CP base metal. It means that the brazed joint has similar property to  $\alpha+\beta$  Ti which is responsible for increasing strength even equal to the base metal.

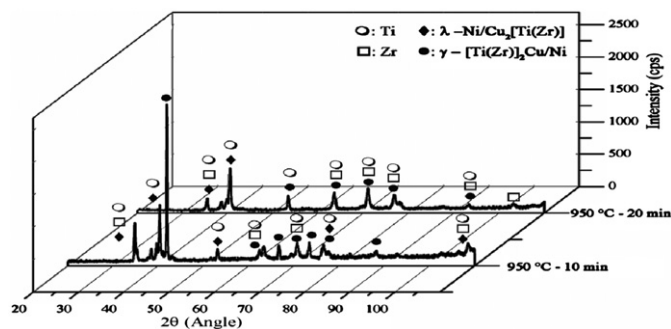


Fig. 10. XRD patterns from the Ti-6Al-4V fractured surfaces which brazed at brazing temperatures of 950 °C for 10 and 20 min.

Table 5  
Microhardness measurement (mean values) at different zones for both substrates at brazing temperature of 870 °C for the Ti-CP and 950 °C for the Ti-6Al-4V.

Base metal	Brazing time	Micro hardness (HV 0.1)						
		BM	IFL	IML	CR	IML	IFL	BM
Ti-CP	10	140	383	572	720	580	480	165
	20	150	488	493	730	493	493	155
	30	152	480	477	483	465	491	143
Ti-6Al-4V	10	491	572	824	1018	839	680	480
	20	460	580	620	710	575	590	480
	30	421	450	515	520	514	464	450

BM (base metal), IFL (interface layer), IML (intermediate layer), CR (central region).

The microhardness results of the Ti-6Al-4V brazed joints with STEMET 1228 at temperature of 950 °C (10–30 min) are shown in Table 5. The microhardness measurements across the brazed joint at 10 min showed the highest level (~720–1010 HV) which indicates to original filler alloy. These are very hard and brittle phases. Intermediate zone between the substrate and the center region revealed 650–840 HV hardness value. Acicular  $\alpha+\beta$  phase at the interface (~572 HV) had a higher hardness than the Ti-6Al-4V base metal (491 HV) with a typical equiaxed  $\alpha+\beta$  microstructure. Acicular features are harder than equiaxed because it is one of martensite transformation [3]. The high hardness of the intermetallic compounds at the center of brazed joint reduces the ductility and hence the allowable plastic deformations which can contribute to decreasing the shear strength of the joints [7]. The microhardness of the brazed joint at 30 min indicates normal values distribution across the whole joint area. Therefore, developing an acicular Widmanstätten structure is useful for improvement of mechanical properties. It is another reason of increasing in strength even equal to the base metals.

3.6. Fractography

Fractographic analysis is a useful method for studying crack nucleation and propagation during shear test. Most of the mechanisms that discuss on the various fracture modes, are based on the concepts of dislocation interactions and movement, involving crystallographic relationships, slip behavior and plastic deformation [39].

To reveal the joint fracture path from the shear test, the shear tested specimens were re-assembled and the cross section of the joint observed by metallography examination. Fig. 11 shows LOM cross-sections and SEM back scattered electron images (BEIs) fractographs after shear test at temperature of 870 °C for 10 and 20 min. The cracks initiated and propagated along the brazed joint, especially along the segregation central region. Pseudo-cleavage fracture with some tearing rapture of the base metal is conspicuously observed in Fig. 11(a) and (b). Increasing the brazing time to 20 min (Fig. 11(c) and (d)) caused to move the crack path to center of brazed joint with dominant brittle fracture which was discussed earlier at Fig. 7. It is obvious that the existence of (Ti,Zr)Cu<sub>2</sub>, (Ti,Zr)<sub>2</sub>Ni and (Ti,Zr)<sub>2</sub>Cu phases were detrimental to shear strength of the joint. With increasing brazing time to 30 min, the fracture path changed from the brazed joint into the substrate.

Fig. 12 shows the cross sections of the Ti-6Al-4V brazed joints with various brazing conditions after the shear test. The fracture path propagated through the brazed joint for the specimen brazed at temperature of 950 °C for 10 min with fully brittle fracture morphology owing to segregated center region. The presence of the Zr-Cu-Ni segregated center region deteriorated the mechanical bonding strength of the brazed joints. These results clearly showed that a segregated center region should be avoided to obtain a strong and robust joint. Fractured surface at the brazing

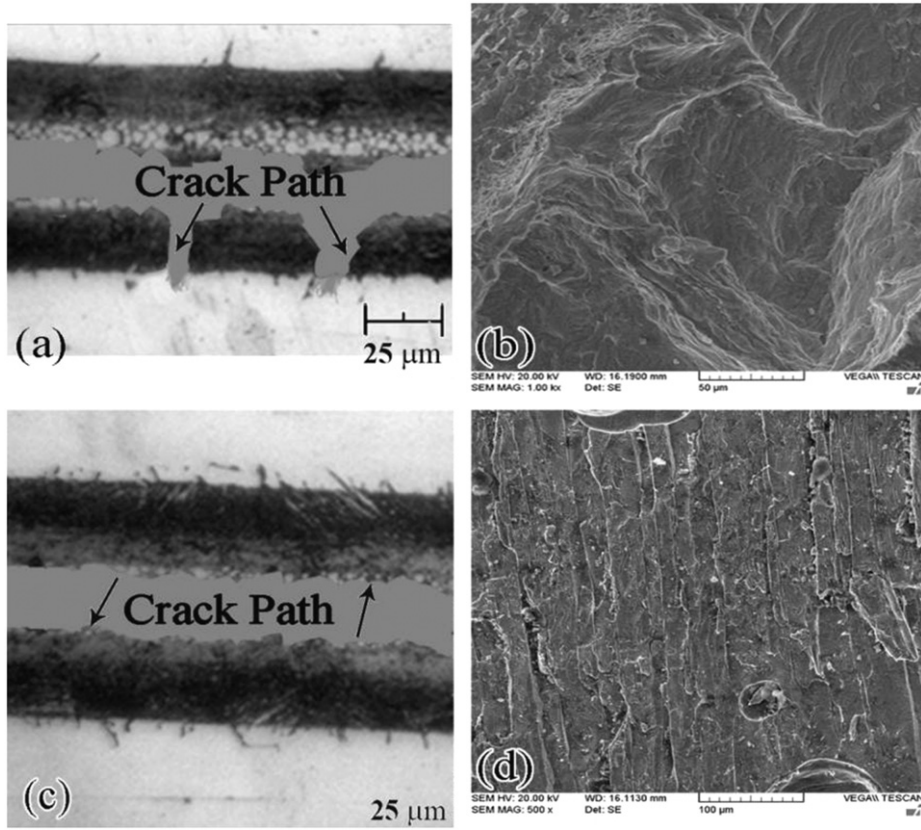


Fig. 11. LOM images displaying cross-section with SEM-BELs fractograph of the Ti-CP brazed joint at 870 °C for (a) and (b) 10 min and (c) and (d) 20 min.

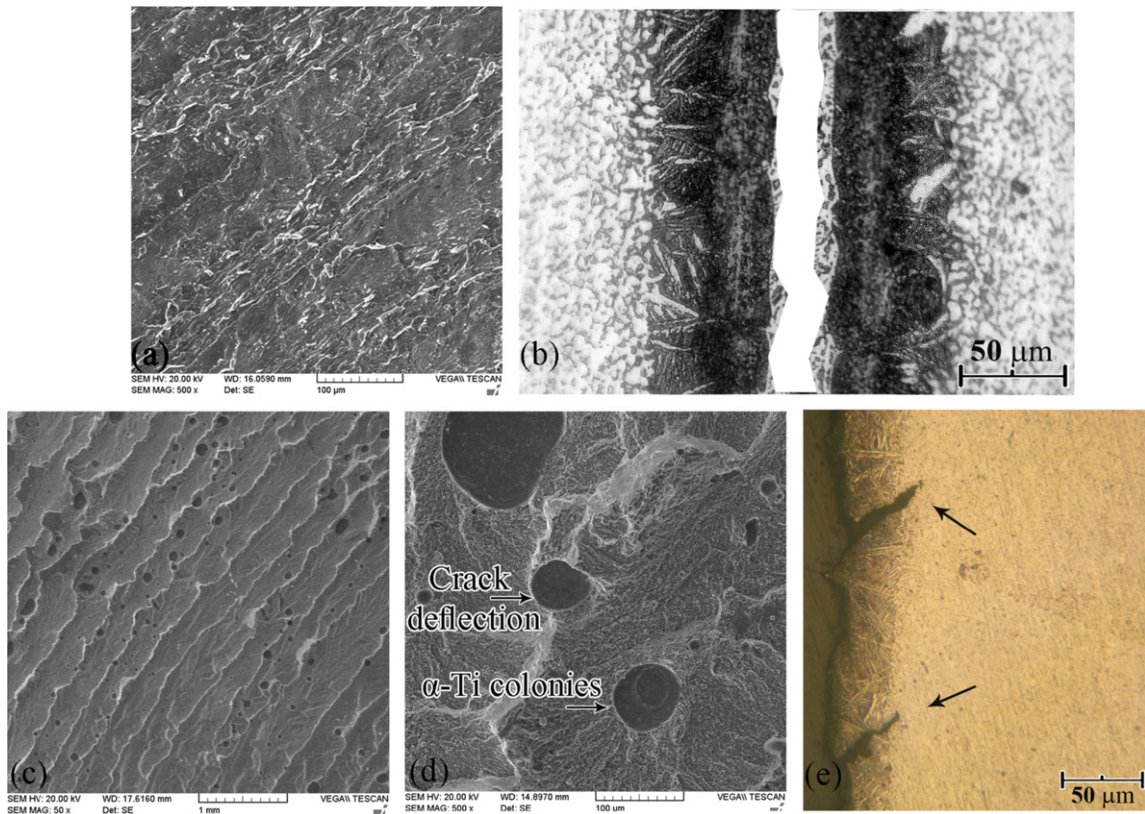


Fig. 12. Fracture morphology and cross-section of the Ti-6Al-4V fracture surface for the joint brazed at a temperature of 950 °C for 10 min (a) and (b) and 20 min (c)–(e).

time of 20 min (Fig. 12(c)), revealed some hole-shape appearance inside river marks (or pearlite) morphology which indicates the brazed joint experienced high plastic deformation before failure [40]. Higher magnification at this hole-shape feature (Fig. 12(d)) shows that these holes maybe are the result of exiting the  $\alpha$ -Ti colonies which were grew from substrate to braze alloy. According to micrograph model from Fig. 3, the  $\alpha$ -Ti colonies had an acicular structure which by prolonging the brazing time, their dimensions became greater. Increasing the applied loading caused these colonies separated from the braze alloy and therefore remained holes on fracture surface. These structures acted as a pin in matter of bonding strength. Fig. 12(d) indicates that the cracks propagated from adjacent of  $\alpha$ -Ti colonies. The  $\alpha$ -Ti phase is more ductile and so the cracks could not to scrape through them. Furthermore, cross-section of fractured surface (Fig. 12(e)) verified these hole-shape indications. Quasi-cleavage fracture is widely observed in specimens with shorter brazing time, e.g., temperature of 950 °C for 20 min instead of brittle dominated morphology.

The fracture path changed from the brazed joint to the substrate for specimens brazed at temperature of 950 °C for 30 min, which had the highest shear strength of 540 MPa. The shear strength measurements and the fracture behaviors recommend that the presences of Cu–Ni and Cu–Ni–Zr rich Ti phases in the brazed joint are detrimental and they should be avoided for obtaining excellent joint.

#### 4. Conclusions

Commercially pure titanium (Ti-CP) and the Ti–6Al–4V alloy have been successfully brazed using STEMET 1228 in a controlled atmosphere furnace. The microstructural development, bonding strength and fractographic analysis were experimentally evaluated. The conclusions are summarized as follows:

- 1- For the STEMET 1228 brazed specimens, the uniformity in element distribution and Widmanstätten structure in brazed region for both substrates are established during the brazing cycle at temperature of 870 °C for the Ti-CP and 950 °C for the Ti–6Al–4V.
- 2- Reaction mechanism showed that upon cooling cycle of brazing, re-solidification of  $\alpha$ -Ti,  $\gamma$ -[(Ti,Zr)<sub>2</sub>Cu/Ni] and  $\lambda$ -Laves (Ni,Cu)<sub>2</sub>[Ti,(Zr)] phases experienced various forms of morphology namely fine eutectoid, Widmanstätten and segregation region. In this case, completing the eutectoidal reaction yielded acicular Widmanstätten structure which was responsible for high mechanical properties.
- 3- The highest average shear strength of 261.7 and 540 MPa, which were equal to the strength of the base metal, were achieved for the Ti-CP and the Ti–6Al–4V, respectively. The joints fractured in the base metal for brazing time of 30 min.
- 4- Several intermetallic compounds such as  $\gamma$ -[(Ti,Zr)<sub>2</sub>Cu/Ni] and  $\lambda$ -Laves (Ni,Cu)<sub>2</sub>[Ti,(Zr)] phases were detected and confirmed by XRD analysis. Lowering intermetallic compounds especially the  $\lambda$  phase were the main reason for increased joint strength. Hence, inordinate formation of hard and brittle intermetallic phases ( $\gamma$  and  $\lambda$  phases) was the fracture mainspring.
- 5- Increasing 80 °C in brazing temperature for the Ti–6Al–4V substrate in order to generating the same microstructure was associated to metallurgical and chemical concepts such as having more surface energy for the Ti–6Al–4V. It means the more energy needed (heat) for rupture the atom bonds in a crystal structure for activating them to do reaction.
- 6- Acicular Widmanstätten structure which was yielded for both brazed substrates has most uniformity in the hardness distribution (465–491 and 450–520 HV for the Ti-CP and the Ti–6Al–4V, respectively) across the whole joints. The hardness of the Ti-CP brazed joints was higher than the base metal.
- 7- From fractography point of view, the pseudo-cleavage fracture with some tearing rapture of the Ti-CP base metal at temperature of 870 °C for 10 min was observed. Increasing the brazing time to 20 min caused to moving the crack path into the center of brazed joint with dominant brittle fracture. Quasi-cleavage fracture observed in specimens brazed with shorter brazing time (20 min) instead of brittle dominated morphology (10 min).
- 8- Fracture path changed from the brazed joint to substrate for both brazed substrates at 30 min. The shear strength measurements and the fracture behaviors proposed that the presences of Cu–Ni or Cu–Ni–Zr rich phases (segregated region) in the brazed joint are detrimental and they should be avoided for achieving appropriate joint.

#### Acknowledgement

The authors would like to appreciate the Physical and Mechanical Properties Laboratory in Faculty of Biomedical Engineering at AUT and Faculty of Aerospace Engineering at KNTU for cooperation and providing the experimental facilities. The authors also gratefully acknowledge the valuable collaboration from Dr. A. Zolriasatein, Dr. E.H. Dehkordi and Eng. M. Heydarifar, NDT PCN Level 3, Iran Air NDT Organization.

#### References

- [1] A. Elrefaey, W. Tillmann, *J. Mater. Sci.* 45 (2010) 4332–4338.
- [2] A. Elrefaey, W. Tillmann, *J. Mater. Sci.* 42 (2007) 9553–9558.
- [3] M.J. Donachie, *TITANIUM: A Technical Guide*, second ed., ASM, USA, 2000.
- [4] C.N. Elias, J.H.C. Lima, R. Valiev, M.A. Meyers, *JOM* (2008).
- [5] B. Cantor, H. Assender, P. Grant, *Aerospace materials*, IOP, 2001.
- [6] V.N. Moiseyev, *Titanium Alloys Russian Aircraft and Aerospace Applications*, Taylor & Francis Group, 2006.
- [7] A. Elrefaey, W. Tillmann, *J. Alloy. Compd.* 487 (2009) 639–645.
- [8] A. Elrefaey, W. Tillmann, *J. Mater. Process. Technol.* 209 (2009) 4842–4849.
- [9] M.M. Schwartz, *Brazing*, second ed., ASM, USA, 2003.
- [10] A. Shapiro, A. Rabinkin, *Weld. J.* (2003) 36–43.
- [11] G. Jiang, D. Mishler, R. Davis, J.P. Mobley, J.H. Schulman, *J. Biomed. Mater. Res. Part B* 72B (2005) 316–321.
- [12] M. Iijima, W.A. Brantley, I. Kawashima, N. Baba, S.B. Alapati, T. Yuasa, H. Ohno, I. Mizoguchi, *J. Biomed. Mater. Res. Part B* 79B (2006) 137–141.
- [13] C.T. Chang, Z.Y. Wu, R.K. Shiue, C.S. Chang, *Mater. Lett.* 61 (2007) 842–845.
- [14] D.H. Kang, J.H. Sun, D.M. Lee, S.Y. Shin, H.S. Kim, *Mater. Sci. Eng. A* 527 (2009) 239–244.
- [15] J.G. Lee, G.H. Kim, M.K. Lee, C.K. Rhee, *Intermetallics* 18 (2010) 529–535.
- [16] R.K. Shiue, S.K. Wu, Y.T. Chen, C.Y. Shiue, *Intermetallics* 16 (2008) 1083–1089.
- [17] C.T. Chang, Y.C. Du, R.K. Shiue, C.S. Chang, *Mater. Sci. Eng. A* 420 (2006) 155–164.
- [18] K. Matsu, Y. Miyazawa, T. Ariga, in: *The Preliminary Program for Third International Brazing And Soldering Conference (IBSC)*, San Antonio, April 23–26, 2006, pp. 70–78.
- [19] M. Materials Science International Team, *Ternary Alloy Systems: Phase Diagrams, Crystallographic and Thermodynamic Data*, Volume 11, Springer, Berlin, Germany, 2007.
- [20] O. Botstein, A. Schwarzman, A. Rabinkin, *Mater. Sci. Eng. A* 206 (1995) 14–23.
- [21] O. Botstein, A. Rabinkin, *Mater. Sci. Eng. A* 188 (1994) 305–315.
- [22] M. Iijima, W.A. Brantley, I. Kawashima, N. Baba, S.B. Alapati, T. Yuasa, H. Ohno, I. Mizoguchi, *J. Biomed. Mater. Res. Part B: Appl. Biomater.* 79B (2006) 137–141.
- [23] JISZ3192, in, 1988.
- [24] E. Ganjeh, H. Sarkhosh, H. Khorsand, H. Sabet, E.H. Dehkordi, M. Ghaffari, *Mater. Des.* 39 (2012) 33–41.
- [25] AWSC3.8, in, 1997.
- [26] *Metals Hand Book*, Vol 9: Metallography and Microstructures, ASM, USA, 1998.
- [27] J.G. Lee, Y.H. Choi, J.K. Lee, G.J. Lee, M.K. Lee, C.K. Rhee, *Intermetallics* 18 (2010) 70–73.
- [28] O. Botstein, A. Shwartzman, A. Mats, J. Danan, in: *Second International Brazing & Soldering Conference (IBSC)*, San Diego, California, February 16–19, 2003.
- [29] G. Lutjering, J.C. Williams, *Titanium*, second ed., Springer, Berlin, 2007.

- [30] Metals Hand Book, Vol 3: Alloy Phase Diagrams, ASM, 1992.
- [31] N. Eustathopoulos, M.G. Nicholas, B. Drevet, *Wettability at High Temperatures*, Pergamon, Oxford, UK, 1999.
- [32] I.T. Hong, C.H. Koo, *Mater. Chem. Phys.* 94 (2005) 131–140.
- [33] A. Meier, P.R. Chidambaram, G.R. Edwards, *Acta. Mater.* 46 (1998) 4453–4467.
- [34] D.A. Porter, K.E. Easterling, *Phase Transformation in Metals and Alloys*, second ed., Chapman & Hall, London, 1992.
- [35] F. Aqra, A. Ayyad, *Appl. Surf. Sci.* 257 (2011) 6372–6379.
- [36] T.A. Roth, P. Suppayr, *Mater. Sci. Eng.* 35 (1978) 187–196.
- [37] J.A. Olmsted, G.M. Williams, *Chemistry*, fourth ed., John Wiley & Sons, USA, 2005.
- [38] D.W. Liaw, Z.Y. Wu, R.K. Shiue, C.S. Chang, *Mater. Sci. Eng. A* 454–455 (2007) 104–113.
- [39] G.E. Dieter, *Mechanical Metallurgy*, third ed., Mc Graw hill, USA, 2001.
- [40] Metals Hand Book, Vol 12: Fractography, ASM, USA, 1987.
- [41] E. Ganjeh, H. Sarkhosh, M.E. Bajgholi, H. Khorsand, M. Ghaffari, *Mater. Charact.* 71 (2012) 31–40.
- [42] M. Ghaffari, P.Y. Tan, M.E. Oruc, O.K. Tan, M.S. Tse, M. Shannon, *Catal. Today* 161 (2011) 70–77.